RESEARCH ARTICLE

Heavy Metals and Arsenic in Sediments of Xinfengjiang Reservoir and East River in South China: Levels, Source and Health Risk Assessment

Yun-jiang Yu[1*†], **Liang-zhong Li**[1†], **Ming-yang Li**[1,2], **Xiao-hui Zhang**[1,3], **Zong-rui Li**[1], **Xiao-hui Zhu**[1], **Bi-gui Lin**[1]

[1] State Environmental Protection Key Laboratory of Environmental Pollution Health Risk Assessment, South China Institute of Environmental Sciences, Ministry of Ecology and Environment, Guangzhou, 510655, China

[2] The College of Natural Resources and Environment of South China Agricultural University, Guangzhou, 510655, China

[3] College of Resources and Environment, Yangtze University, Wuhan, 430100, China

[†] These authors contributed equally to this work

Abstract: Xinfengjiang Reservoir (XFJR) is the largest drinking water source in the southern China, and plays a vital role in supporting the development of China's Pearl River delta. The levels, source identification, potential ecological risks and health risk of eight metal elements including Zn, Pb, Ni, Mn, Cu, Cr, Cd and As in the sediments of the XFJR and Heyuan section of the East River (HYER) were investigated. Sixteen sediment samples were collected from June to July 2016 in XFJR and HYER, and the concentrations of heavy metals (Zn, Pb, Ni, Mn, Cu, Cr, Cd) and As were analyzed simultaneously. Results showed that the total contents of Zn, Pb, Ni, Mn, Cu, Cr, Cd and As in surface sediment of XFJR were 76.27, 36.63, 12.23, 293.61, 14.88, 60.38, 0.76 and 18.68 mg/kg, respectively, and were 76.47, 30.95, 24.47, 361.95, 23.80, 91.81, 0.68 and 7.31 mg/kg, respectively, for HYER. The pollution's levels of the heavy metals and As were in the order of Cd > Zn > Cr > Mn > As > Cu > Ni > Pb. The spatial distribution pattern of heavy metals and As in the surface sediments of the studied area featured high concentrations in the north-eastern region and low concentrations in the XFJR, with a gradual decrease along the river flow from north to south. The results of principal component analysis indicated that agricultural activities, industrial pollution and water vehicles were the main sources of heavy metals pollution. The potential ecological risk index of the region was 22.02, and the potential ecological risk of heavy metals and As were in the ordered of Ni > Cu > Pb > Cr > Zn > Mn > Cd > As, indicating a slight ecological risk. In addition, the non-carcinogenic risk and carcinogenic risk of heavy metal and As in the surface sediment for adult and children were within acceptable level.

Keywords: Heavy metals, surface sediments, source identification, risk assessment

1 Introduction

With the acceleration of urbanization process and the increase of human activities, heavy metal (HMs) pollution has caused great environmental concern and become a risk to ecosystem and public health (Sun et al., 2019; Xu et al., 2019). Human activities produce industrial emissions, municipal waste disposal, and abusive usage of chemical fertilizers and pesticides, leading to an accumulation and sink of HMs in various environmental media (Liu et al., 2020), including sediment which is commonly known to be the major source for HMs (Huang, 2019; Tian et al., 2020). Heavy metals can be released through a series of physical, chemical and biological processes and entered into interstitial and overlying water, resulting in "secondary contamination" (Zhang et al., 2018; Yang et al., 2016). Previous studies show HMs in sediments mainly derive from the long-term effects of natural factors and human production activities including mining activities, agriculture fields, and atmospheric deposition(Chen et al., 2019; Kang et al., 2019). When environmental conditions change, these sediments can also be potential sources of HMs for various aquatic organisms, allowing HMs to enter the food chain (Liu et al., 2020; Zhuang et al., 2019), leading to serious health threat to benthos, aquatic plants and animals, and human (Chon et al., 2012; Yao et al., 2006), due to the high toxicity, non-degradability of HMs to organisms(Chen et al., 2019; Liu et al., 2019). Exposure to Cd mainly leads to kidney damage, chronic cadmium poisoning. Patients even appear nerves, immune and reproductive system damage and tumor occurrence(Park et al., 2019). Pb mainly accumulates in the kidneys, liver and central nervous system, Excessive intake will affect cognitive ability, damage neurobehavioral, especially for children (Nawab et al., 2018). Thus, it is

urgent to investigate the status of HM pollution in sediments, assess the ecological risks and evaluate the potential sources in the XFJR and HYER.

XFJR, also known as Wanlv Lake, is the largest lake in southern China, which located in the western part of Heyuan city, Guangdong Province(Zhao et al., 2007). As drinking water source, XFJR supplies more than 40 million permanent urban residents in Hong Kong and Guangdong Province, such as Heyuan, Huizhou, Dongguan, Shenzhen and Guangzhou. In recent years, with the industrial transfer of the Pearl River Delta, Heyuan has seven industrial transfer industrial parks, including Shenzhen (Heyuan) Industrial Transfer Industrial Park, Shenzhen Bao'an (Longchuan) Industrial Transfer Park, Shenzhen Longgang (Zijin) Industrial Transfer Industrial Park, Shenzhen Yantian (Dongyuan) Industrial Transfer Industrial Park, Shenzhen Futian (peace) industrial transfer industrial park, Shenzhen Dapeng (Heyuanyuancheng) Industrial Transfer Industrial Park, Shenzhen Nanshan (Lianping) Industrial Transfer Park, and Heyuan Jiangdong New Area Industrial Transfer Industrial Park have been planning and building. Transfered industries mainly are electronic appliances, machinery manufacturing, and metal building materials (Yavar et al., 2019), which may discharge heavy metals and other pollutants during production process, causing atmosphere, water and soil pollution (Zhuang et al., 2019; Xu et al., 2019). However, very little information has been reported on HMs in the sediments of XFJR and HYER so far.

In this study, 16 sediment samples were collected in XFJR and HYER, to assess the heavy metal pollution characteristics, ecological and human health risk. The objectives were as follows: (1) to investigate the spatial distribution characteristics of HMs(Zn, Pb, Ni, Mn, Cu, Cr, Cd) and As, (2) to identify the possible sources of metal element using correlation and principle component analyses, (3) to evaluate the pollution degree and ecological risk through geo-accumulation index and potential ecological risk index, (4) to assess human health risk.

2 Materials and methods

2.1 Sample collection

From June to July 2016, 16 sediment samples were collected in XFJR and HYER (6 samples in XFJR and 11 samples in HYER). The sampling sites and XFJR and HYER are shown in Figure 1. Beeker core sampler was used to collect sediment samples. All samples were placed into polyethylene bags and immediately transported to laboratory. Sediment were dried at room temperature and passed through a 100 mesh sieve to remove gravel and coarse debris, and were stored in plastic bags for chemical analysis.

2.2 Sample treatment

About 0.50 g dried sample was digested in Teflon tubes and treated for 30 min in a microwave heating device (MARS6 Xpress) using 10mL of HCl:HNO$_3$ (3:1, v/v). After digesting and cooling, the digested samples were filtered through a 0.45 mm membrane and then diluted to 50ml with 1% HNO$_3$ to 100 ml for further analysis. The concentrations of HMs were analyzed by Agilent 700-ES inductive coupling plasma emission spectrograph (ICP-OES) of Agilent Technologies in Santa Clara, California, USA. The detection limits were $\leqslant$ 8 ng/L and the recoveries ranged between 91 and 110%.

2.3 Assessment methods

2.3.1 Geo-accumulation index

Geo-accumulation index (I$_{geo}$) evaluate the concentration of metals or pollution levels quantitatively by using the total content of metals element and the geochemical background value of As and HMs, and was originally proposed by Müller (Müller et al., 1971), according to the range of I$_{geo}$ values, standard can be divided into 0-6 levels, as detailed in Table 1S.

The I$_{geo}$ calculation formula is as follows:

$$I_{geo} = log_2\left[\frac{C_n}{kb_n}\right] \qquad (1)$$

Where, C_n is the concentration of the metal element n (mg/kg), k is the meter ampere constant used to correct sedimentary features, rock geology and other possible changes in the rock 1.5, and b_n is the geochemical background value (mg/kg) of the metal element n, and the corresponding value of the b_n in this study is from the heyuan urban area of Guangdong Province.
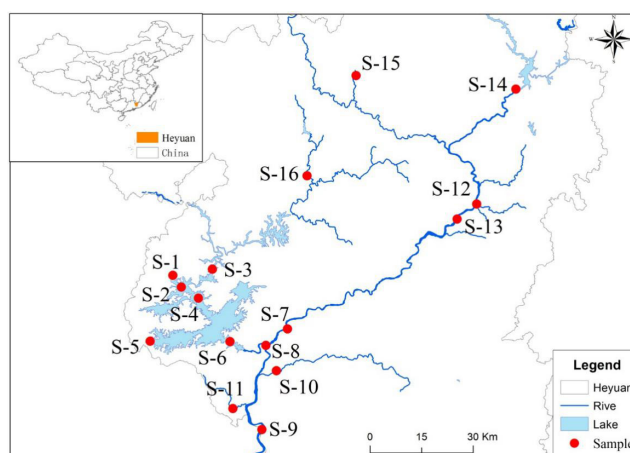

Figure 1. Distribution map of sampling sites

2.3.2 Potential ecological risk

The potential ecological risk index method proposed by Hakanson takes the heavy metal content, species and sensitivity of water bodies to heavy metal pollution in sediments into account to reflect potential ecological risk degree of the

environment of pollutants in sediments (Håkanson, 1980). The potential ecological hazard index coefficient for a single heavy metal is calculated as follows:

$$E_r^i = T_i \times \frac{C_i}{B_i} \qquad (2)$$

In above formula, C_i is the measured amount of the first heavy metal in the sediment; Bi is the evaluation reference value for heavy metals, E_r^i is the potential ecological hazard factor for a single heavy metal; and T_i is the toxicity response parameter for a single pollutant. The cumulative index of potential ecological hazards of a variety of heavy metals is calculated as: RI $= \sum E_r^i$; RI is the potential ecological hazard factor for a variety of heavy metals, The risk rating for the heavy metal risk index (E_r^i and RI) in the sediment are listed in Table 2S.

2.3.3 Human health risk assessment

2.3.3.1 Exposure assessment
To evaluate health risk posed by metals element, the Environmental Protection Agency of the United States risk assessment protocol (USEPA 2004) was used to estimate the risk of inhabitant due to As and heavy metals in sediments of the XFJR and HYER. In general, for heavy metals in sediment, ingestion and dermal absorption are widely considered the main exposure paths (Yavar et al., 2019). The average daily doses (ADDs) of individual metals received through ingestion and dermal contact for both children and adults can be estimated as (Yang et al., 2019).

$$ADDingest = \frac{C \times Ring \times EF \times ED}{BW \times AT} \qquad (3)$$

$$ADDdermal = \frac{C \times SA \times AF \times ABS \times EF \times ED}{BW \times AT} \qquad (4)$$

where C represents the concentration of heavy metal (mg/kg), and other figures (EF, ED, SA et al.) and its values presented in Table 3S.

2.3.3.2 Risk characterization

2.3.3.2.1 Non-carcinogenic risks
In this study, non-carcinogenic risks were estimated using the hazard quotient (HQ)(unit-less) and the hazard index (HI) as followed:

$$HQ = \frac{ADD}{RfD} \qquad (5)$$

$$HI = \sum HQ \qquad (6)$$

where RfD is the reference dose, which is the maximum permissible risk of heavy metals to human health, and its values are listed in Table 4S. HI is the cumulative potential non-carcinogenic risk posed by heavy metals due to multiple routes, is defined as the sum of HQs. For HI < 1, no chronic effects were believed to occur, where as HI > 1 indicated a probability of adverse health effects (USEPA 1989).

2.3.3.2.2 Carcinogenic risks

The carcinogenic risk (CR) is defined as the probability of an individual developing cancer in the whole lifetime exposure to carcinogenic hazards. The CR for an individual over a lifetime could be estimated as followed:

$$CRi = ADDi \times SF \qquad (7)$$

$$TCR = \sum CRi \qquad (8)$$

where SF (dimensionless) is the carcinogenic slope factor (Table 4S); The cancer risk value for regulatory purposes in the range of 10^{-6} to 10^{-4} demonstrates acceptable or tolerable carcinogenic risk. CR value which is higher than 10^{-4} indicates that individuals have a high possibility of developing cancer due to lifetime exposure. CR value $< 10^{-6}$ means no significant cancer risk (USEPA 1989).

2.4 Quality Control
Each batch of samples is added to the procedure blank sample, parallel sample. The detection and analysis of heavy metals is carried out according to national standards, technical specifications and methods provided by the U.S. Environmental Protection Agency. The accuracy of sample analysis is 0.9995, and the relative standard deviation of parallel samples is less than 10%. While analyzing the sediments of XFJR and HYER, we used the same steps to synchronously analyze the heavy metal content of quality control samples (about 10% of the total sample) GBWO/7405-1 to test and control the quality of the analysis data.

2.5 Data Processing
All measured data in this study was analyzed using the software package SPSS 22.0 for Windows. Correlations among As and heavy metals concentrations in the sediment samples were estimated by spearman's correlation coefficients. The KMO (Kaiser-Meyer-Olkin) and Bartlett's tests of sphericity were used to estimate the data suitability for the PCA with our non-normally distributed dataset. The GIS software named ArcMap(version 10.0) is used to carry out the analysis of geostatistics, and the origin V 9.0 is used to draw the charts.

3 Results and Discussion

3.1 Levels of heavy metals in sediments

The HMs and As content in surface sediment of XFJR and HYER was shown in Table 1. The mean concentrations of Zn, Pb, Ni, Mn, Cu, Cd, Cr and As were 76.62, 34.97, 16.41, 332.76, 17.72, 75.31, 0.73, and 13.76 mg/kg, respectively. Mn showed the highest mean value, followed by Zn, Cu, Pb, Cd, Ni, As and Cr. The coefficient of variations (CVs) of HMs and As in the two regions ranged from 32% to 67%, exhibiting moderate to high variation in the study area. The lowest and highest CVs, which were those for Zn and As, respectively. The high CVs found for some HMs indicated that the concentrations of these metals differed greatly at

Table 1 Summary of HMs and As content in HYER and XFJR

	Elements	As(mg/kg)	Cd(mg/kg)	Cr(mg/kg)	Cu(mg/kg)	Mn(mg/kg)	Ni(mg/kg)	Pb(mg/kg)	Zn(mg/kg)
	Range	1.37 − 39.5	0.36 − 1.79	22.58 − 153.55	4.94 − 29.39	134.68 − 594.81	3.38 − 19.75	18.62 − 50.87	34.25− 106.18
XFJR	Mean value	18.68 ±12.56	0.76 ± 0.40	60.38 ±35.10	14.88 ±7.02	293.61 ±142.26	12.23 ± 5.13	36.63 ±12.47	76.27 ± 24.04
	CV (%)	67	53	58	47	48	42	34	32
	Range	2.01 ~ 11.04	0.19 ~ 1.10	18.66 ~ 180.65	7.66 ~ 42.33	121.16 ~587.02	5.14 ~ 42.46	9.52 ~ 58.22	40.38 ~ 109.09
HYER	Mean value	7.31 ± 2.96	0.68 ± 0.30	91.81 ± 53.79	23.80 ± 12.19	361.95 ± 163.75	24.47 ± 12.20	30.95 ± 15.54	76.47 ± 24.26
	CV (%)	41	44	59	51	38	50	50	32

Table 2 I_{geo} value of HMs and As in the sediments

Sample sites	As(I/R)[a]	Cd(I/R)	Cr(I/R)	Cu(I/R)	Mn(I/R)	Ni(I/R)	Pb(I/R)	Zn(I/R)	I_{geo}-AVG(8)[b]	Rank-SUM(8)[c]
S-1	0.49/1	2.61/3	-0.54/0	-0.53/0	-1.52/0	-0.51/0	-1.02/0	-0.54/0	-0.20	0
S-2	1.56/2	3.43/4	-0.26/0	0.21/1	-0.26/0	-0.13/0	-0.16/0	0.58/1	0.62	1
S-3	1.32/2	3.39/4	-0.10/0	-1.23/0	-0.11/0	-0.95/0	-1.32/0	0.44/1	0.18	1
S-4	1.31/2	2.91/3	-0.22/0	-0.84/0	-1.64/0	-0.64/0	-1.54/0	-1.05/0	-0.21	0
S-5	-1.37/0	2.01/3	-1.47/0	-2.37/0	-1.46/0	-2.06/0	-0.52/0	-0.70/0	-0.99	0
S-6	0.41/1	2.05/3	-1.75/0	-2.10/0	-0.91/0	-2.68/0	-0.14/0	0.08/1	-0.63	0
S-7	0.65/1	2.91/3	-0.36/0	-0.46/0	-0.29/0	-0.62/0	-0.09/0	0.19/1	0.24	1
S-8	-0.23/0	2.51/3	-1.32/0	-0.58/0	-1.12/0	-1.06/0	-1.33/0	0.48/1	-0.33	0
S-9	-1.20/0	3.08/4	-0.68/0	-0.26/0	-0.14/0	-0.59/0	0.11/1	0.49/1	0.10	1
S-10	-0.48/0	3.17/4	0.31/1	0.52/1	-0.35/0	0.98/1	-0.48/0	0.62/1	0.54	1
S-11	-1.04/0	1.04/2	-2.02/0	-1.73/0	-1.79/0	-2.07/0	-2.50/0	-0.81/0	-1.37	0
S-12	-3.28/0	3.08/4	-0.34/0	-0.31/0	-0.01/0	-0.14/0	-0.26/0	0.30/1	-0.12	0
S-13	-1.33/0	4.31/5	1.02/2	-1.43/0	0.51/1	-1.13/0	-0.20/0	0.37/1	0.26	1
S-14	-2.73/0	3.61/4	1.25/0	0.73/1	0.49/1	0.66/1	-0.61/0	0.29/1	0.46	1
S-15	-0.58/0	3.20/4	0.83/1	-0.24/0	-0.26/0	0.24/1	-1.39/0	-0.08/0	0.21	1
S-16	-0.27/0	2.15/3	0.00/0	-0.95/0	-0.04/0	0.23/1	-1.21/0	-0.35/0	-0.05	0
Average	-0.58/0	2.78/3	-0.42/0	-0.76/0	-0.55/0	-0.80/0	-0.86/0	0.02/1	-0.15	0

Note: [a] I/R:I_{geo} /I_{geo} level; [b] Average value of the I_{geo} ; [c] The I_{geo} level of the of total metals

different sites, suggesting that they are likely affected by multiple anthropogenic activities (Liu et al., 2020). The I_{geo} was calculated and is presented in Table 2. Pollution conditions were categorized into seven classes utilizing I_{geo} values. The I_{geo} values of Cr, Mn, As, Cu, Ni, Pb remained in class 0 (unpollution), and that of Zn remained in class 1 (unpolluted to moderate polluted), which demonstrated that the metal contents did not exceed the regional background values. Among the eight metals, Cd exhibited the most severe pollution (moderate to strong polluted). Except for the S-11 sampling point, the pollution level of Cd remained in class range from 3 to 5 The sampling point 13 was extremely-strong polluted by Cd (class 5).

The concentrations of HMs and As in the sediment detected in this study were compared with those previously published studies from other Drinking water sources in china (Table 3). The Zn concentration was much lower than that in other regions, except for Miyun Reservoir in Beijing. Cd, Pb concentrations were similar to those in other regions. Ni, Mn and Cu concentrations were relatively low. As was higher than that of other drinking water source.

## 3.2 Spatial distribution characteristics of heavy metals in sediments

The spatial distribution characteristics of HMs and As in the sediments of XFJR and HYER are shown in Figure 2. The spatial distribution of HMs and As in the sediments was that the upper reaches > lower reaches > HYER. The spatial distribution characteristics of Mn, Ni, Cr, Cu, As and Cd were similar in HYER. There was an increasing trend from the southeast towards the northwest, while The concentration of Pb and Zn revealed an increasing trend from reservoir center towards the southeast and the northwest. The highest concentrations of Mn, Ni, Cr, Cu, As and Cd were close to village and confluence, About Pb and Zn, higher concentrations were observed in the southeast and northwest, where, there were main tourist Wharf in the southeast, its development for nearly 20 years, and a village docked with many fishing boats located in the northwest, indicating its amount is mainly affiliated to diesel combustion emissions.

There was an increasing trend in Mn, Ni, Cr, Cd, Pb and Cu concentration from lower reaches towards the upper reaches in the HYER, the high concentrations of Mn, Ni, Cr and Cu sites close to Shenzhen Longgang (Zijin) industrial transfer

Table 3 Comparisons of HMs and As concentration in surface sediment between XFJR and other sites in China

Project	Zn	Pb	Ni	Mn	Cu	Cr	Cd	As	literature
Caohai Lake, Guizhou	219.18	54.01	33.58	-	20.35	56.16	0.84	15.41	(Zhao et al., 2018)
Miyun reservoir, Beijing	25.21	19.14	-	-	80.46	72.44	0.14	8.94	(Pan et al., 2019)
Yuqiao reservoir, Tianjin	91.2	7.24	-	-	34.23	67.55	0.12	6.07	(Liu et al., 2019)
Zhangze reservoir, Shanxi	92.43	39.54	-	-	44.16	-	1.86	5.14	(Zhang et al., 2019)
Bosten Lake, Xinjiang	141.07	51.26	16.34	430.25	23.25	5.54	0.61	-	(Liu et al., 2019)
Yangcheng Lake, Jiangsu	187.33	34.02	68.72	-	66.54	101.28	0.45	15.85	(Guo et al., 2019)
This study	76.27	36.63	12.23	293.61	14.88	60.38	0.76	18.68	
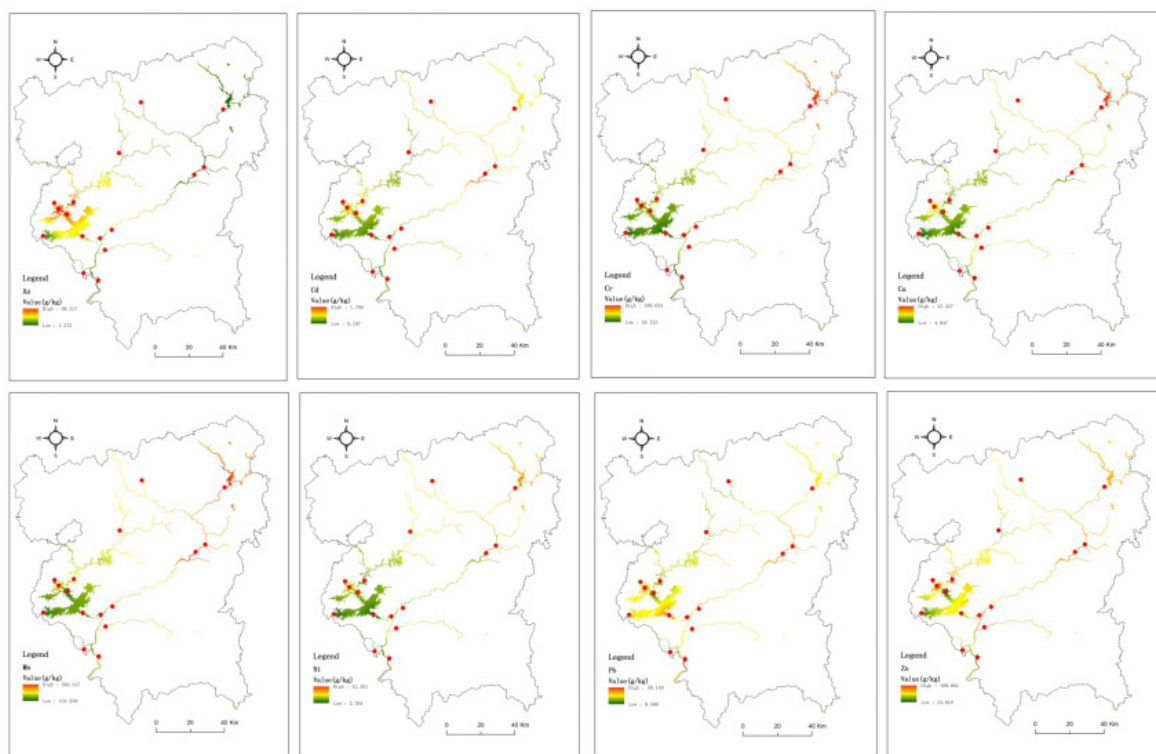
Figure 2. Distribution of HMs and As in Sediments

industrial park, mainly manufacturing electronics, electrical appliances and machinery with the main emissions of pollutants as Cu, Ni, Zn, Cr, etc. The waste water of the sewage treatment plant through the Zhankeng surge (Sewage outlet) enters Baipo River and then into the East River in Linjiang Industrial Zone. Xia et al have shown that industrial emissions were the main source of HMs in water (Xia et al., 2018). Heyuan's dominant wind direction was northeast wind, and the industrial zone was located northeast, resulting in the high concentration of heavy metals in the upper reaches of the East River. Lisa Melymuk et al reported that the settlement of HMs was affected directly by dominant wind (Melymuk et al., 2014). About Pb and Zn, higher concentration were observed in the middle and lower reaches of East River, it was particularly in S-7 and S-8 sampling points where near Huyuan city, Shenzhen Yantian (Dongyuan) Industrial Transfer Industrial Park, and partial sewage pipe network along the East River was not fully laid, indicating part of the sewage did not enter the sewage treatment plant, and discharging into water and affecting water quality (Zhao et al., 2018).

## 3.3 Source identification

The study of the correlation between HMs and As in the sediments revealed that similar pollution was discharged from similar sources (Robertson et al., 2003). The results showed in Table4, the significant correlation of Cr with Cu, Ni, Mn, Cd demonstrated that these HMs were from similar pollution sources, a significant correlation between Cu and Ni (r = 0.864), Cd and Mn (r = 0.789). In contrast, As showed weak positive or negative correlation with other metal elements, suggesting that As originated from another source. the principal component analysis (PCA) was used to analyze the source of HMs and As. The results have been shown in Table 5S and Figure 3. The HMs and As sources in the sediments could be represented by three principal components, the cumulative contribution rate was 82.66% The first principal component (PC1) accounted for 50.11%, Cd, Cr, Cu, Mn and Ni were loaded heavily in PC1, the loads of Cd, Cr, Cu, Ni and Mn were 0.783, 0.898, 0.751, 0.740 and 0.885 respectively. Results above were consistent with the Pearson correlation analysis. Previous studies showed that Ni and

Table 4   Correlation analysis

| Elements	As	Cd	Cr	Cu	Mn	Ni	Pb
As	1						
Cd	0.005	1				.	
Cr	-0.23	0.774**	1				
Cu	-0.07	0.332	0.554*	1			
Mn	-0.262	0.789**	0.794**	0.447	1		
Ni	-0.16	0.264	0.609*	0.864**	0.456	1	
Pb	-0.095	0.355	0.05	0.207	0.42	0.026	1

Note: ** Significant correlation at 0.01 level (bilateral), * Significant correlation at 0.05 level (bilateral).

Cr were related to the parent rock, natural weathering and soil erosion, and mostly from geological minerals in the sediment parent materials (Facchinelli et al., 2001). Irshad et al showed that Cd was an iconic element of symbol element of chemical fertilizer and pesticide (Irshad et al., 2020). There were some industrial parks near XFJR and HYER, including Shenzhen Longgang (Zijin) industrial transfer industrial park and Linjiang Industrial Zone and and other industrial transfer industrial park, which had wastewater treatment plants (WTPs). The enterprises were involved in electronic appliances, machinery manufacturing, metal building materials and other industries. The east river was the main river to received industrial, agricultural and domestic sewage. Moreover, Atmospheric bulk deposition of HMs to the XFJR and HYER. Thus, the overall distribution trend of the Cd, Cr, Cu, Ni and Mn was characterized by high concentrations in the near villages, cities and industrial parks. So, PC1 originated from comprehensive source, including industrial activities, agricultural activities, urban development and natural localization. The second principal component (PC2) accounted for 18.18%, Pb, Cd and Zn were loaded heavily in PC2, the loads of Pb, Cd and Zn were 0.626, 0.437 and 0.430, respectively. Previous studies reported that Cd, Zn and Pb possible sources have been linked to vehicular and ship emissions (Aljahdali et al., 2020). Agricultural activities (fertilizers and pesticides) were important factors contributing to Cd and Pb concentrations in sediments. Thus, PC2 might be derived from vehicular and ship emissions and agricultural activities. The third principal component (PC3) accounted for 14.37%, As was loaded heavily in PC3. The loads of As was 0.961, mainly from the geological process.
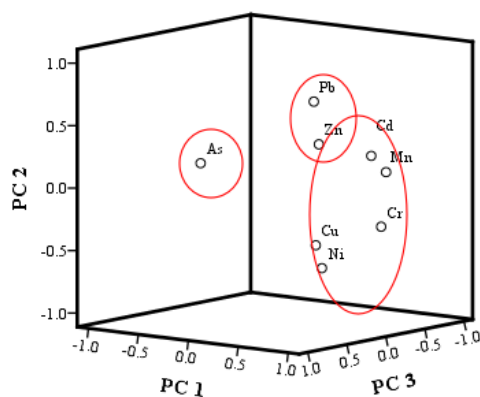

Figure 3. Principal component analysis chart

3.4   Risk assessment

3.4.1   Ecological risk assessment
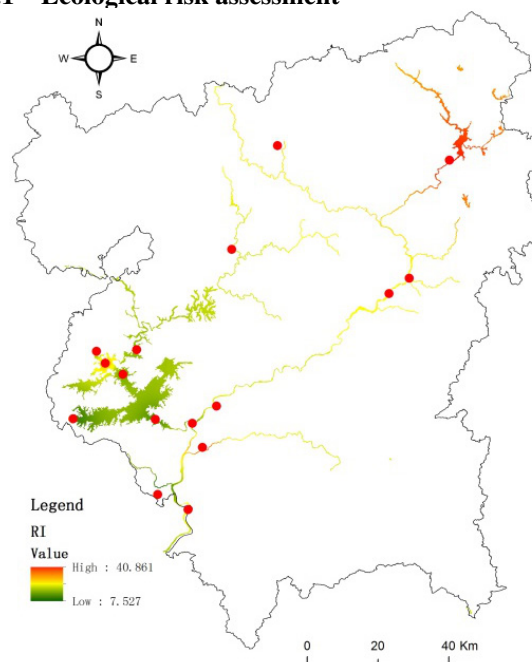
Figure 4. Ecological risk of XFJR and HYER

Potential ecological risk index (RI) method was used to estimate ecological risk of HMs and As in sediments of XFJR and HYER (Table 6S). The Eir values of As (0.002 - 0.044), Cd (0.099 - 0.959), Cr (0.739 - 7.154), Cu (1.452 - 12.450), Mn (0.434 - 2.132), Ni (1.173 - 14.744), Pb (1.323 - 8.087) and Zn (0.724 - 2.306) in each site showed slight risk. The Eir values of individual HMs and As decreased in the order of Ni > Cu > Pb > Cr > Zn > Cd > As. The Eir of HMs and As were lower than 40, which was defined as low ecological risk level in XFJR and HYER, while the geological accumulation index method indicated that the HMs pollution decreased in the order of Cd > Zn > Cr > Mn > As > Cu > Ni > Pb. The attribution to the I_{geo} method mainly reflected the enrichment degree of exotic HMs, which could only suggest the degree of enrichment of single heavy metal by human activities, regardless of the combined effects of bioavailability or HMs(Yang et al., 2019), while the RI method take into consideration the effects of different metal toxicity on organisms(Cao et al., 2018). The coefficient of toxicity of Ni was 14, which was higher than that of several other metals (e.g. Cd, 0.1). Therefore, Cd had a higher degree
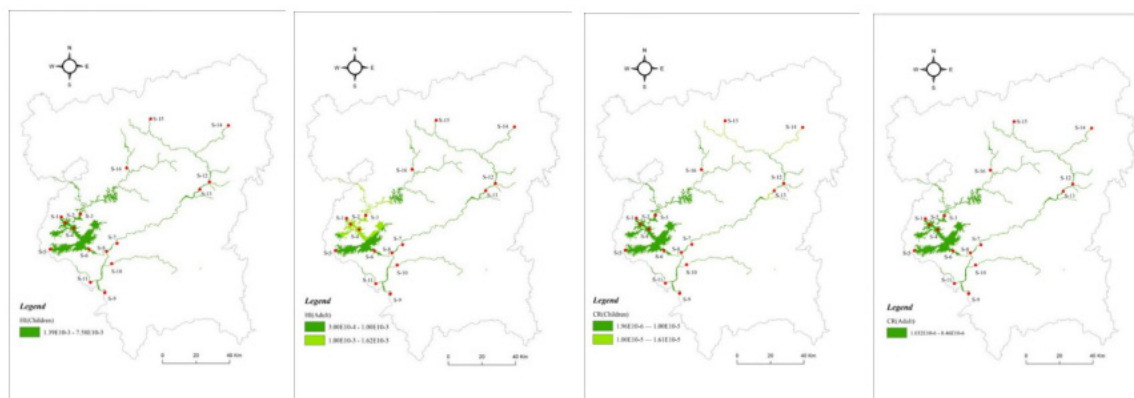
Figure 5. Carcinogenic and non-carcinogenic risk of HMs and As in surface sediment for children and adults living near the XFJR and HYER

of exogenous enrichment, and Ni had a greater ecological risk. The RI value in the XFJR and HYER were 7.50 - 40.86 for HMs and As in the sediment, which was lower than 150 as low integrated potential ecological risk level. The spatial variation of the integrated RI was shown in Figure 4. The RI of HYER was higher than that of XFJR. The highest RI value of HMs was 40.86 , which is similar Fengshu Dam area (upper reaches of East River), probably because of the dam's interception and spillage effect (Li et al., 2020).

3.4.2 Health risk assessment

The non-carcinogenic risks and carcinogenic risks caused by exposure to HMs and As through ingestion and dermal contact for children and adults living near the XFJR and HYER region were shown in Table 6S and Figure 5. For non-carcinogenic risks, the HQ values of As, Cd, Cr, Cu, Mn, Ni and Zn for children and adults were much lower than the acceptable level (HQ = 1). The HQ of HMs and As for multi-pathway exposure were As > Cd > Cr > Mn > Ni > Pb > Cu > Zn for children, and As > Cd> Cr > Mn > Pb > Ni > Cu > Zn for adults. The possibility of exposure to HMs and As in the surface sediment through dermal absorption is higher than ingestion ($HQ_{dermal} > HQ_{ing}$). In addition, the HI values for children varied from1.39E10-3 to 7.58 E10-3, and from 1.62E10-3 to 3.00E10-3 for adult, were particularly lower than the safe level of HI = 1. This displayed no considerable non-carcinogenic risks from the ingestion and dermal contact exposure to HMs and As in surface sediment of XFJR and HYER.

For carcinogenic risk, the CR_{ing} (ingestion carcinogenic risk) in the sediments through ingestion exposure were Cr (1.03E-08) > Ni (8.10E-09) > As(6.13E-09) > Pb (8.31E-11) for children and Cr (1.30E-08) > Ni (1.03E-08) > As(7.77E-09) > Pb (1.05E-10) for adults. Similar to the ingestion route, dermal exposure carcinogenic risk (CR_{dermal}) values for both children and adults decreased in the order of Cr > Ni > As, and were significant higher (p = 0.02) than ingestion carcinogenic risk. This result revealed that dermal contact with surface sediment is the primary route for exposure to toxic metals which could pose a higher carcinogenic risk to local residential. Our results are similar to previous studies (Irshad et al., 2020), which were also within the acceptable level (1×10^{-6} to 1×10^{-4}). The

total human health risks (total CR) were used as the sum of the risks exposed through ingestion and dermal contact. The CR values for children varied from 1.96E10-6 to 1.61E10-5, and from 1.03E10-6 to 8.46 E10-6 for adult, which were also within the acceptable level (1×10^{-6} to 1×10^{-4}), indicating acceptable carcinogenic risk level.

4 Conclusion

This study has shown that the pollution level of HMs in the sediment of XFJR and HYER was related, and the pollution of HMs was from non-polluted to moderate to strong polluted. The principal component analysis and correlation analysis indicated that Cd, Cr, Cu, Mn and Ni were mainly derived from industrial activities, agricultural activities, urban development and natural localization. Industrial activities, vehicular and ship emissions and agricultural activities contributed to the pollution of Pb, Cd and Zn, and the geological process resulting in As contamination. The integrated potential ecological risk level was defined as low ecological risk level of HMs and As in the sediment of XFJR and HYER. In addition, the non-carcinogenic risk and carcinogenic risk of HMs and As in the surface sediment in adult and children were within acceptable level. Although HMs and As contamination in the sediments of XFJR and HYER had a low ecological risk and health risk, long-term dynamic monitoring of HMs and As should be carried out to avoid human health risk and potential ecological risks.

Acknowledgements

References

Aljahdali, M.O., and Alhassan, A.B., 2020. Ecological risk assessment of heavy metal contamination in mangrove habitats, using biochemical markers and pollution indices: A case study of Avicennia marina L. in the Rabigh lagoon, Red Sea. Saudi Journal of Biological Sciences.
https://doi.org/10.1016/j.sjbs.2020.02.004

Cao, Y., Lei, K., Zhang, X., Xu, L., Lin, C. and Yang, Y., 2018. Contamination and ecological risks of toxic metals in the Hai River, China. Ecotoxicology and Environmental Safety, 164, 210-218.
https://doi.org/10.1016/j.ecoenv.2018.08.009

Chen, M., Li, F., Tao, M., Hu, L., Shi, Y. and Liu, Y., 2019. Distribution and ecological risks of heavy metals in river sediments and overlying water in typical mining areas of China. Mar Pollut Bull, 146, 893-899.
https://doi.org/10.1016/j.marpolbul.2019.07.029

Chon, H., Ohandja, D. and Voulvoulis, N., 2012. The role of sediments as a source of metals in river catchments. Chemosphere, 88(10), 1250-1256.
https://doi.org/10.1016/j.chemosphere.2012.03.104

Facchinelli, A., Sacchi, E., and Mallen, L. 2001. Multivariate statistical and GIS-based approach to identify heavy metal sources in soils. Environmental pollution (Barking, Essex : 1987), 114(3), 313-324.
https://doi.org/10.1016/S0269-7491(00)00243-8

Guo, X.Y., Gao, M., Zhang, J., Zhang, H.T., Zhu, J.G. and Deng, J.C., 2019. Characteristics of spatial distribution andbiological toxicity for heavy metals in sediments of the Yangcheng Lake. China Environmental Science 39(2), 802-811.

Håkanson, L. 1980. An ecological risk index for aquatic pollution-control-A sedimentological arrroach. Water Res, 14, 975-1001.
https://doi.org/10.1016/0043-1354(80)90143-8

Huang, B. 2019. Changes in chemical fractions and ecological risk prediction of heavy metals in estuarine sediments of Chunfeng Lake estuary, China. Mar Pollut Bull, 138, 575-583.
https://doi.org/10.1016/j.marpolbul.2018.12.015

Irshad, M.K., Noman, A., Alhaithloul, H.A.S., Adeel, M., Rui, Y., Shah, T., Zhu, S. and Shang, J., 2020. Goethite-modified biochar ameliorates the growth of rice (Oryza sativa L.) plants by suppressing Cd and As-induced oxidative stress in Cd and As co-contaminated paddy soil. Science of the Total Environment, 717.
https://doi.org/10.1016/j.scitotenv.2020.137086

Kang, J., Zhou, L., Duan, X., Sun, H., Ao, Z. and Wang, S., 2019. Degradation of Cosmetic Microplastics via Functionalized Carbon Nanosprings. Matter, 1(3), 745-758.
https://doi.org/10.1016/j.matt.2019.06.004

Li, Y., Gao, B., Xu, D., Peng, W., Liu, X., Qu, X. and Zhang, M., 2020. Hydrodynamic impact on trace metals in sediments in the cascade reservoirs, North China. Science of the Total Environment, 716.
https://doi.org/10.1016/j.scitotenv.2020.136914

Liu, M., Chen, J., Sun, X., Hu, Z. and Fan, D., 2019. Accumulation and transformation of heavy metals in surface sediments from the Yangtze River estuary to the East China Sea shelf. Environmental Pollution, 245, 111-121.
https://doi.org/10.1016/j.envpol.2018.10.128

Liu, P., Hu, W., Tian, K., Huang, B., Zhao, Y., Wang, X., Zhou, Y., Shi, B., Kwon, B.O., Choi, K., Ryu, J., Chen, Y., Wang, T. and Khim, J.S., 2020. Accumulation and ecological risk of heavy metals in soils along the coastal areas of the Bohai Sea and the Yellow Sea: A comparative study of China and South Korea. Environ Int, 137, 105519.
https://doi.org/10.1016/j.envint.2020.105519

Liu, Z.L., Yan, Y.J., Lu, J.J., Liu, J.H. and Chen, B.M., 2019. Pollution characteristics and pollution degree assessment of heavy metals in surface sediments from Bosten Lake. Journal of Shihezi University (Natural Science), 37(5), 613-620.

Melymuk, L., Robson, M., Csiszar, S.A., Helm, P.A., Kaltenecker, G., Backus, S., Bradley, L., Gilbert, B., Blanchard, P., Jantunen, L, and Diamond, M. L., 2014. From the City to the Lake: Loadings of PCBs, PBDEs, PAHs and PCMs from Toronto to Lake Ontario. Environmental Science & Technology, 48(7), 3732-3741.
https://doi.org/10.1021/es403209z

Müller, G., 1979. Heavy metals in sediment of the Rhine-changes since 1971. Umschau in Wissenschaft Und Technik, 79, 778-783.

Nawab, J., Khan, S. and Xiaoping, W., 2018. Ecological and health risk assessment of potentially toxic elements in the major rivers of Pakistan: General population vs. Fishermen. Chemosphere, 202, 154-164.
https://doi.org/10.1016/j.chemosphere.2018.03.082

Pan, L., Wu, R., Wang, L., Wang, Y., Fang, G., Su, B., Wang, S. and Xiang, B., 2019. Heavy metal pollution levels and risk assessment of soils and sediments in the upstream of Miyun Reservoir, Beijing. Journal of environmental engineering technology, 9(3), 261-268.

Park, J., Lee, S., Lee, E., Noh, H., Seo, Y., Lim, H., Shin, H., Lee, I., Jung, H., Na, T. and Kim, S.D., 2019. Probabilistic ecological risk assessment of heavy metals using the sensitivity of resident organisms in four Korean rivers. Ecotoxicol Environ Saf, 183, 109483.
https://doi.org/10.1016/j.ecoenv.2019.109483

Robertson, D.J., Taylor, K.G. and Hoon, S.R., 2003. Geochemical and mineral magnetic characterisation of urban sediment particulates, Manchester, UK. Applied Geochemistry, 18(2).
https://doi.org/10.1016/S0883-2927(02)00125-7

Sun, C., Zhang, Z., Cao, H., Xu, M. and Xu, L., 2019. Concentrations, speciation, and ecological risk of heavy metals in the sediment of the Songhua River in an urban area with petrochemical industries. Chemosphere, 219, 538-545.
https://doi.org/10.1016/j.chemosphere.2018.12.040

Tian, K., Wu, Q., Liu, P., Hu, W., Huang, B., Shi, B., Zhou, Y., Kwon, B.O., Choi, K., Ryu, J., Seong Khim, J. and Wang, T., 2020. Ecological risk assessment of heavy metals in sediments and water from the coastal areas of the Bohai Sea and the Yellow Sea. Environment International, 136.
https://doi.org/10.1016/j.envint.2020.105512

USEPA 1989. Risk Assessment Guidance for Superfund, Volume 1: Human Health Evaluation Manual (Part a), Interim Final. U.S. Environmental Protection Agency, Office of Emergency and Remedial Response. Washington, 1-288.

USEPA 2004. Risk Assessment Guidance for Superfund Volume I: Human Health Evaluation Manual (Part E, Supplemental Guidance for Dermal Risk Assessment).

Xia, F., Qu, L., Wang, T., Luo, L., Chen, H., Dahlgren, R.A., Zhang, M., Mei, K. and Huang, H., 2018. Distribution and source analysis of heavy metal pollutants in sediments of a rapid developing urban river system. Chemosphere, 207.
https://doi.org/10.1016/j.chemosphere.2018.05.090

Xu, X., Wang, T., Sun, M., Bai, Y., Fu, C., Zhang, L., Hu, X. and Hagist, S., 2019. Management principles for heavy metal contaminated farmland based on ecological risk-A case study in the pilot area of Hunan province, China. Sci Total Environ, 684, 537-547.
https://doi.org/10.1016/j.scitotenv.2019.05.015

Yang, C., Wu, Y., Zhang, F., Liu, L. and Pan, R., 2016. Pollution characteristics and ecological risk assessment of heavy metals in the surface sediments from a source water reservoir. Chemical Speciation & Bioavailability, 28(1-4), 133-141. https://doi.org/10.1080/09542299.2016.1206838

Yang, F., Zhang, S., Sun, Y., Du, Q., Song, J. and Tsang, D.C.W., 2019. A novel electrochemical modification combined with one-step pyrolysis for preparation of sustainable thorn-like iron-based biochar composites. Bioresource Technology, 274, 379-385. https://doi.org/10.1016/j.biortech.2018.10.042

Yao, Z. 2006. Environmental geochemistry of heavy metals in sediments of Dongting Lake. Geochimica, 35(6), 629-638.

Yavar Ashayeri, N., and Keshavarzi, B. 2019. Geochemical characteristics, partitioning, quantitative source apportionment, and ecological and health risk of heavy metals in sediments and water: A case study in Shadegan Wetland, Iran. Mar Pollut Bull, 149, 110495. https://doi.org/10.1016/j.marpolbul.2019.110495

Zhang, Q., Feng, M.Q. and Hao, X.Y., 2019. Pollution characteristics and ecological risk assessment of heavy metals in the sediments of zhangze reservoir. Environmental engineering, 37(1), 11-17.

Zhang, Z., Lu, Y., Li, H., Tu, Y., Liu, B. and Yang, Z., 2018. Assessment of heavy metal contamination, distribution and source identification in the sediments from the Zijiang River, China. Science of The Total Environment, 645, 235-243. https://doi.org/10.1016/j.scitotenv.2018.07.026

Zhao, B., Zhu, S., Yang, X., Wang, M., Su, C. and Xu, C., 2018. Pollution Status and Ecological Risk Assessment of Heavy Metals in Sediments of Caohai Lake. Research of environmental sciences, 32(2), 235-224.

Zhao, G., Ye, S., Yuan, H., Ding, X., Wang, J. and Laws, E.A., 2018. Surface sediment properties and heavy metal contamination assessment in river sediments of the Pearl River Delta, China. Marine Pollution Bulletin, 136, 300-308. https://doi.org/10.1016/j.marpolbul.2018.09.035

Zhao, S.Y. and Han, B.P., 2007. Structural analysis of zooplankton community in a large deep oligotrophic reservoir-Xinfengjiang Reservoir, South China. Journal of Lake Sciences, 19(3), 305-314. https://doi.org/10.18307/2007.0312

Zhuang, W., Ying, S.C., Frie, A.L., Wang, Q., Song, J., Liu, Y., Chen, Q. and Lai, X., 2019. Distribution, pollution status, and source apportionment of trace metals in lake sediments under the influence of the South-to-North Water Transfer Project, China. Science of The Total Environment, 671, 108-118. https://doi.org/10.1016/j.scitotenv.2019.03.306

Supplementary information

Table 1S   Geoaccumulation index and classification of pollution degree

I_{geo}	Degree	Pollution level
$\leqslant 0$	0	Unpolluted
0 - 1	1	Unpolluted to moderately polluted
1 - 2	2	Moderately polluted
2 - 3	3	Moderately to strongly polluted
3 - 4	4	Strongly polluted
4 - 5	5	Strongly to very strongly polluted
$\geqslant 5$	6	Very strongly polluted

Table 2S   Potential ecological risk coefficients

Range	Risk Level of single Pollutant	Range	Comprehensive potential ecological risk level
$E_r^i < 40$	Slight	RI<150	Slight
$40 \leq E_r^i < 80$	Medium	$150 \leq RI < 300$	Medium
$80 \leq E_r^i < 160$	Strong	$300 \leq RI < 600$	Strong
$160 \leq E_r^i < 320$	Very strong	$600 \leq RI$	Very strong
$320 \leq E_r^i$	Extremely strong	/	/

Table 3S   Exposure factors

Steps	Formulation/symbol/unit	Value	Ref
the concentration of each metal	C	-	-
exposure frequency (day/year)	EF	350	US EPA(2001)
exposure duration (year)	ED	30 years for adults and 12 years for children	MEP (2016)
the surface area of the skin (cm^2)	SA	Adults:3300; children: 2800	US EPA(2001)
the skin adherence factor(mg/cm^2)	AF	0.2	US EPA(2001)
the dermal absorption factor	ABS	0.001	US EPA(2001)
body weight(kg)	BW	57.2 (adults); 29 (children)	MEP (2016)
average time (day)	AT	AT=ED×365 days for non-carcinogens and AT=25550 days for carcinogens	US EPA(2001)

Note: MEP (Ministry of Environment Protection), 2016. Exposure factors handbook of Chinese population, China Environmental Science Press; US EPA (United States Environmental Protection Agency), 2001. Risk assessment Guidance for super-fund. Process for Conducting Probabilistic Risk Assessment (Volume III-Part A, 540-R-502-002)

Table 4S Summary of trace metal toxicological characteristics

Metal	Oral RfD[a] (mg·kg⁻¹·day⁻¹)	Dermal RfD[c] (mg·kg⁻¹·day⁻¹)	Oral SF[a,b] (mg·kg⁻¹·day⁻¹)	Dermal SF[a,d] (mg·kg⁻¹·day⁻¹)
Pb	1.40E-03	NF	8.50E-03	NA
Cd	1.00E-03	2.50E-05	NA	NA
Ni	2.00E-02	5.40E-03	1.70E+00	4.25E+01
Cu	4.00E-02	1.20E-02	NA	NA
Zn	3.00E-01	6.00E-02	NA	NA
Mn	1.40E-01	2.33E-02	5.01E-01	2.00E+01
Cr	3.00E-03	3.00E-03	NA	NA
As	5.00E-03	1.23E-04	1.50E+00	3.66E+00

Note: NF: No Found; NA-not applicable. [a] US EPA (United States Environmental Protection Agency), 1999. Risk Assessment Guidance for Super-fund, Volume (Part A: Human Health Evaluation Manual; Part E, Supplemental Guidance for Dermal Risk Assessment; Part F, Supplemental Guidance for Inhalation Risk Assessment).http://www.epa. gov/ oswer/ risk assessment/ human health exposure. htm; [b] US EPA (United States Environmental Protection Agency), 2011. The screening level (RSL) tables (Last updated June 2011). (available on-line at http://www.epa.gov/region 9/superfund/prg/index.html; [c] Cao, S., Duan, X., Zhao, X., Wang, B., Ma, J., Fan, D., Sun, C., He, B., Wei, F., Jiang, G., 2015. Health risk assessment of various metal(loid)s via multiple exposure pathways on children living near a typical lead-acid battery plant, China. Environmental pollution 200, 16-23; [d] Duan, X.L., Wang, Z.S., Li, Q., Zhang, W.J., Huang, N., Wang, B.B., Zhang, J.L., 2011. Health risk assessment of heavy metals in drinking water based on field measurement of exposure factors of Chinese People. Environ. Sci. 32(5), 1329-1339.

Table 5S Load and contribution rate of variable principal components analysis

Element	Principle component		
	1	2	3
As	-0.255	0.002	0.961
Cd	0.783	0.437	0.249
Cr	0.898	-0.044	0.016
Cu	0.751	-0.476	0.122
Mn	0.885	0.313	-0.056
Ni	0.74	-0.602	0.013
Pb	0.357	0.626	-0.042
Zn	0.701	0.43	0.335
Total	3.917	1.38	1.093
variance (%)	48.96	17.25	13.66
Accumulation (%)	48.96	66.21	79.87

Table 6S Non-carcinogenic and carcinogenic risks of heavy metals in the sediment from XFJR and HYER

	Risk	As	Cd	Cr	Cu	Mn	Ni	Pb	Zn
Children									
	HQ_ing	4.77E-06	1.21E-06	3.98E-05	7.53E-07	3.77E-06	1.39E-06	4.07E-05	4.21E-07
	HQ_dermal	2.17E-03	5.42E-04	4.45E-04	2.81E-05	2.54E-04	5.77E-05	-	2.36E-05
Non-carcinogenic	HI_ing	9.28E-05							
	HI_dermal	3.50E-03							
	HI	3.60E-03							
	CRing	6.13E-09	-	1.03E-08	-	-	8.10E-09	8.31E-11	-
carcinogenic	CR_dermal	1.67E-07	-	4.58E-06	-	-	2.27E-06	-	-
	TCR	1.41E-05							
Adults									
	HQing	2.41E-06	6.13E-07	2.02E-05	3.82E-07	3.77E-06	7.05E-07	2.07E-05	2.13E-07
	HQ_dermal	4.54E-04	1.13E-04	9.32E-05	5.88E-06	5.31E-05	1.21E-05	-	4.93E-06
Non-carcinogenic	HI_ing	4.89E-05							
	HI_dermal	7.36E-04							
	HI	7.85E-04							
	CR_ing	7.77E-09	-	1.30E-08	-	-	1.03E-08	1.05E-10	-
carcinogenic	CR_dermal	8.76E-08	-	2.40E-06	-	-	1.19E-06	-	-
	CR	7.40E-06							